

Least-Squares Fitting of a Three-Dimensional Ellipsoid to Noisy Data

Alexandra Malyugina, Konstantin Igudesman, Dmitry Chickrin

Kazan Federal University,
35 Kremlyovskaya St., Kazan 420008, Republic of Tatarstan, Russian Federation

Copyright © 2014 Alexandra Malyugina, Konstantin Igudesman and Dmitry Chickrin. This is an open access article distributed under the Creative Commons Attribution License, which permits unrestricted use, distribution, and reproduction in any medium, provided the original work is properly cited.

Abstract

This paper deals with the problem of fitting a three-dimensional ellipsoid to a noisy data point set in the context of three-axis magnetometer calibration. It describes methods of ellipsoidal fitting, based on various concepts of ellipsoid representation, error function definition and data simulation. The efficiency of the new approaches is demonstrated through simulations.

Mathematics Subject Classification: 65D15, 65D10

Keywords: ellipsoid fitting, least squares fitting

1 Introduction

Fitting quadric curves and surfaces to point data has been a classical mathematical problem, which has been widely studied because of the wide range of its applications in many areas of science e.g. computer vision, pattern recognition, particle physics, observational astronomy and structural geology. The approach to ellipsoid fitting developed in this article was motivated by its application to magnetometer calibration problem.

Three-axis magnetometers are used to measure the intensity of the Earth magnetic field, and are widely used in navigation systems, aircrafts and many other engineering applications. Unfortunately the data from low cost sensors

can be distorted with various disturbances, including soft- and hard-iron effects. This makes it necessary to perform the sensor calibration just before use. For a calibrated magnetometer the collected data lies on a sphere. The presence of magnetic distortions will cause the magnetometer data to lie on an ellipsoid instead. Thus, estimating parameters of the ellipsoid on which the distorted data lies and accounting for these errors will therefore map the ellipsoid of magnetometer data to a sphere.

Generally, the problem can be formulated as follows: given n cloud points $\mathbf{x}_i = \{x_i, y_i, z_i\}_{i=1}^n$ in three dimensional space that lie on an ellipsoid \mathcal{E}^2 , how can one find \mathcal{E}^2 (i.e. parameters of \mathcal{E}^2)?

The existing methods of ellipsoidal fitting are mainly based on the least-squares method, and can be divided into two groups according to their error definitions. Methods of the first group use an algebraic approach regarding an implicit representation of the quadratic surface

$$F(\mathbf{a}, \mathbf{x}_i) = 0,$$

where \mathbf{a} is a vector of quadratic form coefficients.

The error distance thus can be defined by substituting cloud points' coordinates to the implicit equation and the ellipsoid fitting is proceeded by minimizing the sum of squared distances. The most widely used algorithm in this category was proposed by Fitzgibbon, Pilu and Fisher [5]. It is developed for two-dimensional case and uses algebraic least squares method to the constraint $4ac - b^2 = 1$ (a , b and c are coefficients of quadric equation of an ellipse), that guarantee that the result of the calculation will necessarily appear to be an ellipse. Later this approach was modified in [7] and generalized for the case of spheroids [13]. There are also several algorithms of algebraic curve and surface fitting that use different constraints, e.g. Bookstein's algorithm with a quadratic constraint [2] or its refinement — Sampson's algorithm. Bookstein showed that if a quadratic constraint is set on the parameters, the minimization can be solved by considering a generalized eigenvalue system:

$$D^T D \mathbf{a} = \lambda C \mathbf{a},$$

where $D = [x_1, x_2, \dots, x_n]^T$ is called the design matrix, \mathbf{a} represents a vector of parameters and C is the matrix that expresses the constraint.

B.Bertoni [1] presents an algorithm of ellipsoid fitting that works well for fitting ellipsoids with a known center. It is based on the algorithm of W. C. Karl [9], developed in his article "Reconstructing objects from projection" (1991) and uses lower dimensional projections of the ellipsoid. If the center of the ellipsoid is known, the ellipsoid can be completely represented by a symmetric, positive semi-definite matrix. This allows to get a linear relationship between the positive semi-definite representation of the d-dimensional ellipsoid, and its m-dimensional projection.

Methods of other type use alternative “geometrical” definition of error distance, regarding it as the shortest distance from the data point to the surface. Though geometric methods give better solutions, they require more time for evaluation. Methods using algebraic concept are more reasonable in terms of computational cost. In his article [3] D. Eberly develops methods of hyperplanar fitting and surface fitting for several kinds of quadric curves and surfaces including circles, ellipses, spheres, paraboloids and ellipsoids. Considering the problem of ellipsoidal fitting he focuses on axis-aligned ellipsoid. D. Eberly defines error as normal distance from the point of the cloud to the ellipsoid. The closest point on the ellipsoid is found by a Newton’s iteration scheme.

There are other approaches to ellipsoid fitting that involve minimizing various distance functions, such as “approximate mean square distance metric”, that was introduced by G. Taubin [12]. He defines the distance as follows:

$$\varepsilon^2 = \frac{\sum_{i=1}^n F(\mathbf{a}, \mathbf{x}_i)^2}{\sum_{i=1}^n \|\nabla_X F(\mathbf{a}, \mathbf{x}_i)\|^2}.$$

A statistical approach for the ellipsoid fitting problem was proposed by Kanatani and Porrill in [8] and [10]. Kanatani proposed an unbiased estimation method, called a renormalization procedure. But the noise variance estimate proposed in [8] is still inconsistent; the bias is removed up to the first order approximation. According to comparison, made in [5], complexity level of this algorithm is high.

In this article we construct a number of algebraic fitting methods of a two-dimensional ellipsoid \mathcal{E}^2 into a cloud of noisy data points, using different mathematical representations of ellipsoid and error function definitions. We also test these methods on modelled data, adapting them to various modes of magnetometer sensor positioning. In Section 2 we consider two different ways of representation of a two-dimensional ellipsoid \mathcal{E}^2 , Section 3 is devoted to error distance definitions. In this section we prove the lemma that shows the relation between natural geometric definition of the distance between point and ellipsoid and “algebraic distance”, that is defined by a quadric equation of the ellipsoid. In Section 4 we represent simulated data points that imitate various magnetometer sensor positioning. In the last section we describe the scheme of our algorithms and provide results of calculations.

2 Mathematical representation of an ellipsoid

An arbitrary two-dimensional ellipsoid \mathcal{E}^2 can be regarded as an affine transformation of a unit sphere \mathbf{S}^2 centered in the origin. We can define this affine transformation using nine parameters: semi-axis a, b, c , Euler angles ϕ, ψ, θ of successive rotations about axis and coordinates of the center x_0, y_0, z_0 . Thus,

the affine transformation, that maps a unit sphere \mathbf{S}^2 to an ellipsoid \mathcal{E}^2 can be performed by three matrices of successive rotations $R_1(\phi)$, $R_2(\psi)$, $R_3(\theta)$ over corresponding axis OX , OY and OZ

$$R_1(\phi) = \begin{pmatrix} 1 & 0 & 0 \\ 0 & \cos(\phi) & -\sin(\phi) \\ 0 & \sin(\phi) & \cos(\phi) \end{pmatrix}$$

$$R_2(\psi) = \begin{pmatrix} \cos(\psi) & 0 & -\sin(\psi) \\ 0 & 1 & 0 \\ \sin(\psi) & 0 & \cos(\psi) \end{pmatrix}$$

$$R_3(\theta) = \begin{pmatrix} \cos(\theta) & -\sin(\theta) & 0 \\ \sin(\theta) & \cos(\theta) & 0 \\ 0 & 0 & 1 \end{pmatrix}.$$

Stretching along axis can be represented by a diagonal matrix

$$J(a, b, c) = \begin{pmatrix} a & 0 & 0 \\ 0 & b & 0 \\ 0 & 0 & c \end{pmatrix}.$$

Finally, we can write for affine transformation:

$$\begin{pmatrix} x' \\ y' \\ z' \end{pmatrix} = R_1(\phi) \cdot R_2(\psi) \cdot R_3(\theta) \cdot J(a, b, c) \begin{pmatrix} x \\ y \\ z \end{pmatrix} + \begin{pmatrix} x_0 \\ y_0 \\ z_0 \end{pmatrix}.$$

The inverse transformation is given by

$$\begin{pmatrix} x \\ y \\ z \end{pmatrix} = M \begin{pmatrix} x' \\ y' \\ z' \end{pmatrix} - M \begin{pmatrix} x_0 \\ y_0 \\ z_0 \end{pmatrix},$$

with

$$M = J(1/a, 1/b, 1/c) \cdot R_3(-\theta) \cdot R_2(-\psi) \cdot R_1(-\phi).$$

As a special case of quadric surfaces, an ellipsoid can be described by an implicit second order polynomial. Substituting the expression for (x, y, z) into the equation of the sphere $x^2 + y^2 + z^2 - 1 = 0$, we obtain the quadric equation of the ellipsoid

$$F(\mathbf{a}, x, y, z) = 0,$$

where \mathbf{a} represents the vector of nine parameters of the affine mapping.

Another approach to mathematical representation of an ellipsoid \mathcal{E}^2 involves the use of an upper triangular matrix. We assume, that points on unit sphere \mathbf{S}^2 can be mapped by an affine transformation that is given by

$$\begin{pmatrix} x' \\ y' \\ z' \end{pmatrix} = P \begin{pmatrix} x \\ y \\ z \end{pmatrix} + \begin{pmatrix} x_0 \\ y_0 \\ z_0 \end{pmatrix},$$

with

$$P = \begin{pmatrix} p_{11} & p_{12} & p_{13} \\ 0 & p_{22} & p_{23} \\ 0 & 0 & p_{33} \end{pmatrix}.$$

In the similar way as we did before we can define ellipsoid, substituting transformed coordinates into the equation of \mathbf{S}^2 .

The matrix P is defined by the unique transformation that maps unit sphere \mathbf{S}^2 to the ellipsoid \mathcal{E}^2 . This representation depends on nine parameters and it is equivalent to the first representation.

3 Error distance minimization

Fitting of a general conic may be approached by minimizing the sum of squared error distances.

The most natural way is to consider geometrical representation of error distance. Let $\bar{\mathbf{x}}' = f(\bar{\mathbf{x}})$ be an affine mapping that takes points of \mathbf{S}^2 to points of the ellipsoid \mathcal{E}^2 . Then we consider data points $\{\bar{\mathbf{x}}'_i\}_{i=1}^n$ and define “geometric distance” between the data point $\bar{\mathbf{x}}'_i$ and the ellipsoid \mathcal{E}^2 as

$$\delta(\bar{\mathbf{x}}'_i) = \|\bar{\mathbf{x}}'_i - \bar{\mathbf{y}}'_i\|,$$

where $\bar{\mathbf{y}}'_i$ is the point of intersection of the ellipsoid \mathcal{E}^2 and the line, connecting the center of \mathcal{E}^2 and $\bar{\mathbf{x}}'_i$.

In some cases it is more convenient to calculate error distance using the algebraic representation of an ellipsoid. Substituting data points $\bar{\mathbf{x}}_i$ into the quadric equation of an ellipsoid we can define the distance

$$\varepsilon(\bar{\mathbf{x}}'_i) = F(\mathbf{a}, \bar{\mathbf{x}}'_i), \quad i = \overline{1, n}, \quad (1)$$

that is often called an “algebraic distance” from the surface to the point. We will establish the relation between these two definitions of geometric and algebraic distances in the lemma below.

Lemma. (The relation between geometric and algebraic distances)

Considering $\bar{\mathbf{x}}' = A\bar{\mathbf{x}} + \bar{\mathbf{x}}_0$ an affine mapping, with A a non-degenerate 3×3 matrix, that takes points of the sphere \mathbf{S}^2 to points of the ellipsoid

\mathcal{E}^2 , let $\varepsilon(\bar{\mathbf{x}}'_i)$ and $\delta(\bar{\mathbf{x}}'_i)$ correspondingly be algebraic and geometric distances from the point $\bar{\mathbf{x}}'_i$ to \mathcal{E}^2 defined as above. Then there is the following relation between $\varepsilon(\bar{\mathbf{x}}'_i)$ and $\delta(\bar{\mathbf{x}}'_i)$:

$$\varepsilon(\bar{\mathbf{x}}'_i) = \delta(\bar{\mathbf{x}}'_i) \frac{\|A^{-1}\bar{\mathbf{x}}'_i\|}{\|\bar{\mathbf{x}}'_i\|} (\delta(\bar{\mathbf{x}}'_i) \frac{\|A^{-1}\bar{\mathbf{x}}'_i\|}{\|\bar{\mathbf{x}}'_i\|} + 2)$$

for all points $\bar{\mathbf{x}}_i$ lying inside \mathcal{E}^2 and

$$\varepsilon(\bar{\mathbf{x}}'_i) = \delta(\bar{\mathbf{x}}'_i) \frac{\|A^{-1}\bar{\mathbf{x}}'_i\|}{\|\bar{\mathbf{x}}'_i\|} (\delta(\bar{\mathbf{x}}'_i) \frac{\|A^{-1}\bar{\mathbf{x}}'_i\|}{\|\bar{\mathbf{x}}'_i\|} - 2)$$

for points $\bar{\mathbf{x}}_i$ outside ellipsoid \mathcal{E}^2 .

Proof.

The distances δ and ε between points $\bar{\mathbf{x}}$ on the sphere and preimages $\bar{\mathbf{x}}_i = A^{-1}(\bar{\mathbf{x}}'_i) - A^{-1}(\bar{\mathbf{x}}_0)$ of data points $\bar{\mathbf{x}}'_i$ can be calculated as

$$\delta(\bar{\mathbf{x}}_i) = | \|\bar{\mathbf{x}}\| - 1 |, \quad \varepsilon(\bar{\mathbf{x}}_i) = \|\bar{\mathbf{x}}\|^2 - 1.$$

Therefore

$$\varepsilon(\bar{\mathbf{x}}_i) = (\delta(\bar{\mathbf{x}}_i) + 1)^2 - 1 = \delta(\bar{\mathbf{x}}_i)(\delta(\bar{\mathbf{x}}_i) + 2)$$

for all points $\bar{\mathbf{x}}_i$ lying inside ellipsoid, and

$$\varepsilon(\bar{\mathbf{x}}_i) = (\delta(\bar{\mathbf{x}}_i) - 1)^2 - 1 = \delta(\bar{\mathbf{x}}_i)(\delta(\bar{\mathbf{x}}_i) - 2)$$

for all points $\bar{\mathbf{x}}_i$ lying outside \mathcal{E}^2 .

Recalling that a unit sphere is given by the quadratic form

$$F(\bar{\mathbf{x}}) = \bar{\mathbf{x}}^t \bar{\mathbf{x}} - 1$$

and substituting $\bar{\mathbf{x}} = A^{-1}(\bar{\mathbf{x}}'_i) - A^{-1}(\bar{\mathbf{x}}_0)$, we get a quadratic form

$$F(\bar{\mathbf{x}}') = \bar{\mathbf{x}}^t (A^{-1})^t A^{-1} \bar{\mathbf{x}} - 2 \bar{\mathbf{x}}_0^t (A^{-1})^t A \bar{\mathbf{x}} + \bar{\mathbf{x}}_0^t (A^{-1})^t A^{-1} \bar{\mathbf{x}}_0 - 1,$$

that is equivalent to $F(\bar{\mathbf{x}})$. This implies

$$\varepsilon(\bar{\mathbf{x}}'_i) = \varepsilon(\bar{\mathbf{x}}_i).$$

The geometric distance between data points $\bar{\mathbf{x}}'_i$ and \mathcal{E}^2 can be calculated using geometric distance from data points of the sphere:

$$\delta(\bar{\mathbf{x}}'_i) = \delta(\bar{\mathbf{x}}_i) \frac{\|\bar{\mathbf{x}}'_i\|}{\|\bar{\mathbf{x}}_i\|},$$

from that follows

$$\delta(\bar{\mathbf{x}}_i) = \delta(\bar{\mathbf{x}}'_i) \frac{\|A^{-1}\bar{\mathbf{x}}'_i\|}{\|\bar{\mathbf{x}}'_i\|},$$

and, finally

$$\varepsilon(\bar{\mathbf{x}}'_i) = \delta(\bar{\mathbf{x}}'_i) \frac{\|A^{-1}\bar{\mathbf{x}}'_i\|}{\|\bar{\mathbf{x}}'_i\|} (\delta(\bar{\mathbf{x}}'_i) \frac{\|A^{-1}\bar{\mathbf{x}}'_i\|}{\|\bar{\mathbf{x}}'_i\|} + 2)$$

for all points $\bar{\mathbf{x}}_i$ lying inside \mathcal{E}^2 and

$$\varepsilon(\bar{\mathbf{x}}'_i) = \delta(\bar{\mathbf{x}}'_i) \frac{\|A^{-1}\bar{\mathbf{x}}'_i\|}{\|\bar{\mathbf{x}}'_i\|} (\delta(\bar{\mathbf{x}}'_i) \frac{\|A^{-1}\bar{\mathbf{x}}'_i\|}{\|\bar{\mathbf{x}}'_i\|} - 2)$$

for points $\bar{\mathbf{x}}_i$ outside ellipsoid \mathcal{E}^2 . \square

4 Modelling data points

In our experiments we considered different testing positioning modes of 3-axis magnetometer: rotation around one of its axis, rotation around sphere and moving the sensor along an elliptic path.

To obtain a reasonably plausible model that is to some extent representative and correspond the reality, we used a parametric representation of a sphere \mathbf{S}^2 for data point sets simulation:

$$\begin{cases} x = \cos(u) \sin(v), \\ y = \sin(u) \sin(v), \\ z = \cos(v), \end{cases} \quad \text{with } u \in [0, 2\pi], v \in [0, \pi]$$

For the first experiment we regarded random points that are normally distributed in the space of parameters u, v , with $u \in [0, 2\pi]$, $v \in [0, \pi/3]$. In the second and third cases we considered random points that are situated on the sphere and randomly distributed on some polyline in (u, v) -space. Then for all cases we applied an affine transformation to \mathbf{S}^2 , that simulates hard-iron and soft-iron effects. Illustrations of real data and corresponding modelled data of different modes are provided below.

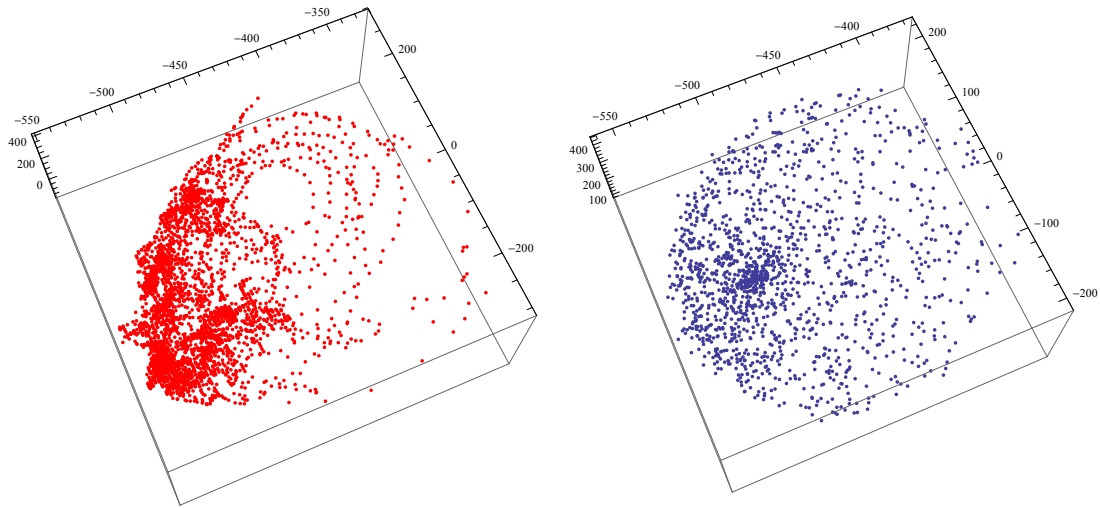


Fig. 1. Magnetometer sensor rotates over one of its axes:

a) real data b) data simulation

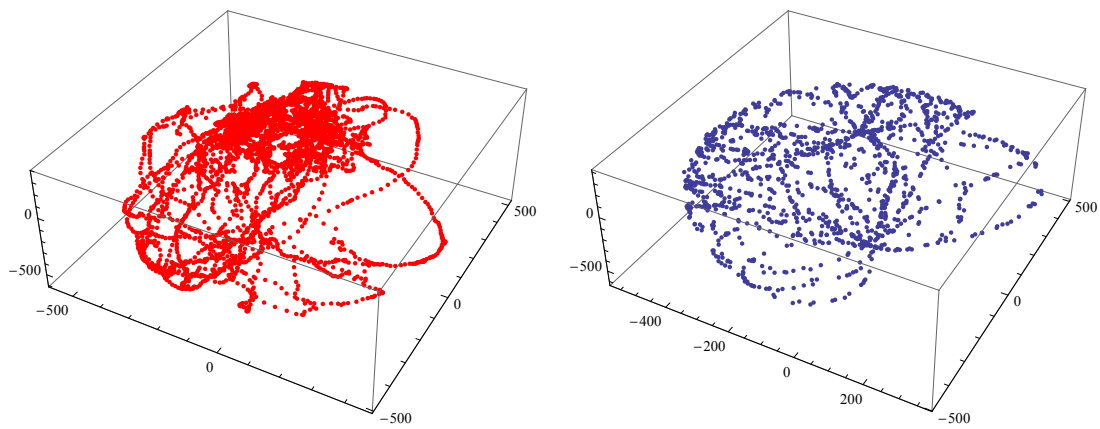


Fig. 2. Magnetometer sensor rotates around center in different planes:

a) real data b) data simulation

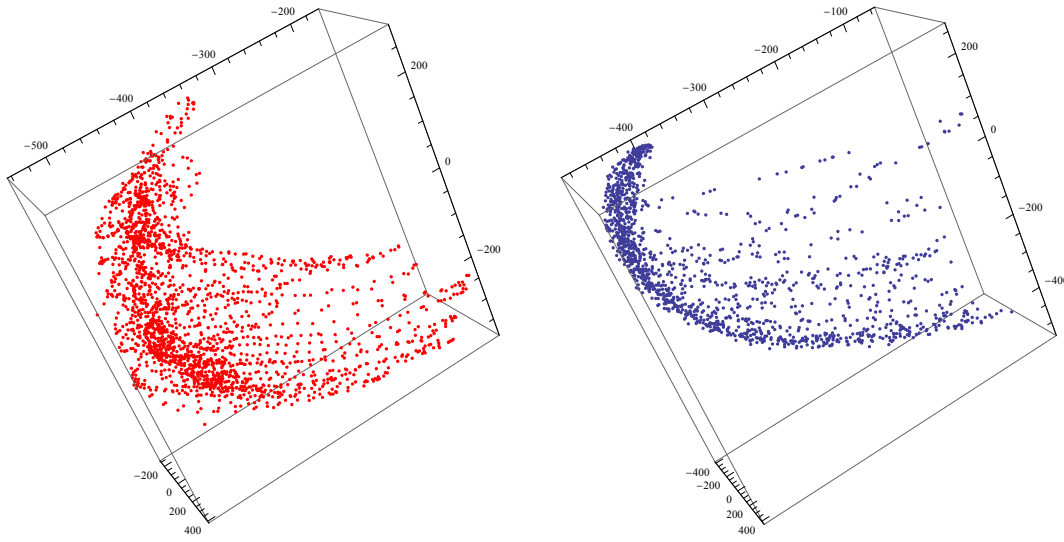


Fig. 3. Magnetometer sensor moves along elliptic path:
a) real data b) data simulation

As a result we have presented computational results that were realized in Wolfram Mathematica 9.0. We used a built-in simulated annealing algorithm for minimization of error functions. Simulated annealing algorithm is an optimisation method that is based on the imitation of the physical process of heated metals cooling. As a metal cools, its atoms fluctuate between high and low energy levels. If the temperature decreases at the speed low enough, the atoms will all reach their ground state. However, if the temperature decreases too quickly, the system will get trapped in a configuration that is worse than optimum. Assuming that the function $E(x)$ to be minimized is analogous to the internal energy of the system in some initial state, the goal of the simulated annealing algorithm is to bring the system from an arbitrary initial state to a state with the minimum possible energy. The algorithm generates the point x_{i+1} from the point x_i in the following way. On the first stage it draws at random a point x^* that becomes the point x_{i+1} with the probability $P(x^*, x_{i+1})$, that can be calculated using Gibbs distribution:

$$P(x^* \rightarrow x_{i+1} | x_i) = \begin{cases} 1, & E(x^*) - E(x_i) < 0 \\ \exp\left(-\frac{E(x^*) - E(x_i)}{T_i}\right), & E(x^*) - E(x_i) \geq 0 \end{cases},$$

where $T_i > 0$ is a sequence, decreasing to zero. T_i can be interpreted as "synthetic temperature" that tends to 0. The main advantages of the simulated annealing algorithm are that it is largely independent of the starting values and that it can escape local minima through selective uphill moves. The reason for choosing simulated annealing algorithm was that it is superior to

simplex method, Adaptive Random Search and quasi-Newton algorithm and some other methods, being evaluated in the space of many parameters.

In order to justify results, all errors need to be normalized. The absolute value of the determinant of the matrix A of affine transformation $f(\mathbf{x}) = A\mathbf{x} + b$ measures the ratio of volume distortion under transformation f . Therefore we consider the coefficient

$$\Delta_p = \frac{1}{|\det A|^{p/3}},$$

where A is a matrix of the affine transformation that maps unit sphere \mathbf{S}^2 to an ellipsoid \mathcal{E}^2 and p is the dimension of the variable under consideration (e.g. we have $p=1$ for axis lengths). Then a normalized error can be defined as follows:

$$\widetilde{err}_p = \Delta_p \times err_p,$$

where err_p is the initial error, calculated for the variable of dimension p .

5 Results and conclusions

We divided the problem of ellipsoid fitting into three stages: mathematical representation of the ellipsoid, error distance calculation and testing the algorithm with modelled data. Using concepts we described in the previous sections we constructed various methods of ellipsoid fitting, combining different concepts on each stage and tested them in different data simulation modes. Abbreviations below stand for different ellipsoid representations, methods of error distance calculation and magnetometer data modelling modes:

Representation of the ellipsoid \mathcal{E}^2 :

Euler — The representation of the ellipsoid \mathcal{E}^2 by its semi-axis a, b, c , Euler angles ϕ, ψ, θ of and coordinates of the center x_0, y_0, z_0 .

Affine — The ellipsoid \mathcal{E}^2 is represented by the upper-triangular matrix and center coordinates x_0, y_0, z_0 .

Minimization of error functions:

p1 — Minimization of the sum of absolute values of algebraic error distances.

p2 — Minimization of the sum of squared algebraic error distances.

Modes of data modelling:

Rotate — Data simulation mode, when magnetometer sensor rotates over one of its axes.

Ell_path — Data simulation mode that represents the movement of the sensor along elliptic path.

Sph_rotate —Data simulation mode imitating rotations around center in different planes.

We evaluated a number of experiments of fitting three-dimensional ellipsoid with given parameters to noisy data of n points, using all possible combinations of representation, error distance definitions and modelled data testing. For the experiment below we considered 1500 points $\mathbf{x}_i = \{x_i, y_i, z_i\}_{i=1}^{1500}$ in three-dimensional space and the ellipsoid with given parameters: semi-axes lengths $a = 1, b = 2, c = 3$, Euler angles $\phi = \frac{\pi}{4}, \psi = \frac{\pi}{3}, \theta = \frac{\pi}{4}$ and coordinates of the center $x_0 = -2, y_0 = 0, z_0 = 1$. Points are represented parametrically and distributed with random noise

$$\begin{cases} x_i = (1 + \alpha) \cos(u) \sin(v), \\ y_i = (1 + \alpha) \sin(u) \sin(v), \\ z_i = (1 + \alpha) \cos(v), \end{cases} \quad \text{with } u \in [0, 2\pi], v \in [0, \pi],$$

where α is a random variable with normal distribution of mean 0 and variance 0.01.

The results of the calculations are presented in the table below.

Method	Center error	Semi-principal axes error
Rotate+euler +p1	1×10^{-2}	$\{5 \times 10^{-4}, 6 \times 10^{-5}, 1.1 \times 10^{-2}\}$
Rotate+euler +p2	1×10^{-2}	$\{6.5 \times 10^{-4}, 5.5 \times 10^{-4}, 1.1 \times 10^{-3}\}$
Ell_path+euler +p1	1.7×10^{-2}	$\{7.3 \times 10^{-4}, 4.8 \times 10^{-4}, 4.1 \times 10^{-3}\}$
Ell_path+euler +p2	1.7×10^{-2}	$\{4 \times 10^{-4}, 3 \times 10^{-2}, 2 \times 10^{-3}\}$
Sph_rotate+euler +p1	2×10^{-3}	$\{1.8 \times 10^{-4}, 1.5 \times 10^{-4}, 1.4 \times 10^{-5}\}$
Sph_rotate+euler +p2	2.4×10^{-3}	$\{1.8 \times 10^{-3}, 1.8 \times 10^{-2}, 2 \times 10^{-4}\}$
Rotate+affine +p1	2×10^{-2}	$\{1.8 \times 10^{-3}, 2.9 \times 10^{-3}, 3 \times 10^{-2}\}$
Rotate+affine +p2	2.2×10^{-2}	$\{2.1 \times 10^{-3}, 3 \times 10^{-3}, 3.3 \times 10^{-2}\}$
Ell_path+affine +p1	5.1×10^{-3}	$\{2.8 \times 10^{-3}, 8 \times 10^{-3}, 5.6 \times 10^{-4}\}$
Ell_path+affine +p2	7.7×10^{-3}	$\{2 \times 10^{-4}, 7 \times 10^{-3}, 2.2 \times 10^{-4}\}$
Sph_rotate+affine +p1	1.7×10^{-3}	$\{6.2 \times 10^{-5}, 3.4 \times 10^{-3}, 5 \times 10^{-5}\}$
Sph_rotate+affine +p2	1.4×10^{-3}	$\{1.8 \times 10^{-3}, 1.6 \times 10^{-3}, 3 \times 10^{-4}\}$

Fig. 4. Computational results

Using proposed methods with noisy data, we obtained reasonably good experimental results showing that these methods can be applied to solving the

problem of ellipsoid fitting. The advantage of these methods is their simplicity and computational efficiency that is a key characteristic of all least-squares algebraic methods. Another essential feature is their independence from constraints that are needed when performing classical least-squares algorithms.

Concerning comparison of all the approaches performed in this article, the best approaches that use the shortest computational time and produce slightly better results than others are the approaches “**Sph_rotate + affine + p1**” and “**Sph_rotate + affine + p2**” that use data from magnetometer sensor that rotates around its center in different planes and mathematical representation of ellipsoid with an upper-triangular matrix of affine transformation.

Acknowledgements. The work was performed according to the Russian Government Program of Competitive Growth of Kazan Federal University as part of the OpenLab Ariadna.

References

- [1] B. Bertoni. Multi-dimensional ellipsoidal fitting, Department of Physics, South Methodist University, Tech. Rep. SMU-HEP-10-14, 2010
- [2] F. L. Bookstein, Fitting conic sections to scattered data, *Comput. Graph. Image Process.*, vol. 9, pp. 56–71, 1979.
- [3] D. Eberly. Least Squares Fitting of Data, Geometric Tools, LLC, 1999
- [4] W. Feng, S.B. Liu, S.W. Liu, S. Yang. A calibration method of three-axis magnetic sensor based on ellipsoid fitting. *J. Inf. Comput. Sci.* 2013, 10, 1551–1558.
- [5] A. W. Fitzgibbon, R. B. Fischer. A buyer’s guide to conic fitting. In *Proc. of the British Machine Vision Conference*, pages 265–271, Birmingham, 1995.
- [6] W. Gander, G. H. Golub, R. Strebler. *Least-Squares Fitting of Circles and Ellipses*, 1994
- [7] R. Halif, J. Flusser. Numerically stable direct least squares fitting of ellipses, in *Proc. Sixth Int Conf. Computer Graphics and Visualization*, 1, pp. 125–132, 1998
- [8] K. Kanatani. Statistical bias of conic fitting and renormalization. *IEEE T-PAMI*, 16(3):320–326, 1994
- [9] W. C. Karl. *Reconstructing Objects from Projections*. PhD thesis, MIT, Dept of EECS, 1991.

- [10] J. Porrill. Fitting ellipses and predicting confidence envelopes using a bias corrected kalman filter. *Image and Vision Computing*, 8(1):37–41, 1990
- [11] P. D. Sampson. Fitting conic sections to very scattered data: An iterative refinement of the bookstein algorithm. *Computer Graphics and Image Processing*, 18:97–108, 1992.
- [12] G. Taubin. Estimation of planar curves, surfaces and nonplanar space curves defined by implicit equations with applications to edge and range image segmentation, *IEEE Trans. Pattern Analysis and Machine Intelligence*. 1991.
- [13] J. Yu, S. R. Kulkarni, H. V. Poor. Robust ellipse and spheroid fitting. *Pattern Recognition Letters*, 33 (5), 492–499, 2012

Received: September 4, 2014; Published: October 23, 2014